24th INTERNATIONAL CONGRESS ON SOUND AND VIBRATION
23–27 July 2017, London

VIBRATION OBSERVATION AND CONTROL FOR THE TIP OF A MOTOR-DRIVEN TRANSLATIONAL FLEXIBLE MANIPULATOR BASED ON OPTIMAL CONTROL ALGORITHM

Li Wei* and Ju Jinyong

School of Mechatronic Engineering, China University of Mining and Technology, Xuzhou 221116, China
email: liweicumt@163.com

The translational flexible manipulator driven by a servo-motor is taken as a study object. Considering the residual vibrations during its locating process, the sensor-less detection of the tip and the vibration suppression of the flexible manipulator are investigated. In order to constitute effective feedback control to suppress the residual vibrations, the vibration signals of the flexible manipulator should be obtained firstly. Because of the low stiffness and large deflection, the introduction of the sensor is bound to affect the dynamic characteristics of the flexible manipulator. Then, based on the lumped parameter dynamic model of the flexible manipulator, a vibration observer is designed to obtain the vibration signals of the translational flexible manipulator by replacing the traditional sensors which are regularly adopted in current control methods. Moreover, the observer gains of the vibration observer are optimized by the optimal control algorithm, which aims to minimize the observation error while keeping the observer stable. Finally, in order to verify the effectiveness of the designed vibration observer, a model of the physical translational flexible manipulator system is constructed by ADAMS, which is regarded as a controlled object, and a state-feedback integral controller is designed to suppress the vibrations. Results show that the designed methods have a noticeable effect of vibration observation during the uniform motion and uniformly accelerated motion of the slider. Furthermore, the designed vibration observer can accurately observe the residual vibration of the tip of the flexible translational manipulator.

Keywords: translational flexible manipulator, vibration observer, state-feedback integral controller, vibration suppression, combined-simulation

1. Introduction

With the high-precision and high-speed development of robots technology, it requires higher demands for mechanical arm [1,2]. Compared with the rigid manipulator, the flexible manipulator has numerous advantages, such as smaller damping, higher speed and larger load. As a consequence, it is increasingly applied in practice. Because of the low modal frequency and small structural damping, the flexible manipulator exhibits a long transient vibration when positions quickly, which seriously impacts the positioning speed and accurate tracking ability. Therefore, the vibration mechanism and control strategy of the flexible manipulator have always been a quite focused issue [3].

The translational flexible manipulator (TFM) is a typical rigid-flexible coupling dynamic system, and has received numerous attentions in the dynamic modelling and control strategies [4]. These control methods can be categorized into passive and active control. Early passive control method is simple and easy to implement, such as employing elastic damping materials to accelerate the vibration attenuation of the TFM. However, as the increasing requirement of control precision for the TFM, the passive control, for the limited control effect and poor adaptability, remains difficult to meet the demands of engineering. Fortunately, the active control technology can effectively suppress the vibrations of the TFM by using the input energy to counteract the system vibration energy,

which has been widely applied. Based on the genetic algorithm, Qiu [5] realized the dynamic adjustment of PD parameters for the trajectory tracking of the cylinder pedestal and the vibration suppression of the flexible manipulator. Malki [6] applied a fuzzy PID controller to the vibration control of the TFM and verified the effectiveness and robustness of this control method. However, in the present research, the sensors must be applied and installed on the manipulator to measure the vibration signals, and subsequently the addition of sensors is bound to affect the dynamic characteristics of the TFM system [7]. Moreover, the performance of the sensors is susceptible to environmental factors which reduce the reliability of the whole system.

Fortunately, the sensor-less technology is becoming a hotspot in the field of high-speed driven system. Yoo [8] designed an adaptive observer for the purpose of observing the link velocity signals of a flexible-joint robot. In order to avoid the influence of the sensors on the small mechanical structure, the control of the cooperative robots without velocity measurements was analysed in [9]. In [10], the trajectory tracking control for a two planar robots is realized while the vibration signals of the operated objects are not measured by physical sensors. Mosayebi [11] proposed a nonlinear high gain observer to estimate the elastic degrees of freedom for input–output control of flexible manipulator. Through appropriate design, the elastic vibration of the flexible manipulator can be well estimated by the state observer [12]. Although, there are many design methods for the observer gains in the existing research, those methods are often used to estimate the state variables of the original system. The sensor-less measurement for the vibration signals of the flexible manipulator has not yet been reported.

Based on the dynamic model and the Luenberger observer, a vibration observer is proposed to measure the vibration signals of the tip for the TFM. Therefore, in order to simplify the design process and realize the optimization of the observation effect, the optimal control algorithm is adopted to design the observer gains. Furthermore, the state feedback control thought combined with integral is adopted to suppress the vibration of the TFM and validates the efficiency of the vibration observer. The remainder of this paper is organized as follows. The dynamic modelling of TFM is given in Section 2. The main contribution of this paper is described in Section 3, including the design of the observer and control strategy. Section 4 provides the union simulations to illustrate effectiveness of the proposed control strategy. Finally, conclusions are drawn in Section 5.

2. Dynamic Modelling of the TFM

Schematic diagram is shown in Fig. 1. The TFM is driven by servo motor and ball screw and it is fixed on the base. During the construction of the dynamic model, assumptions are made that: the TFM is simplified as an Euler-Bernoulli beam by neglecting the impact of shear and axial deformation and the connection between the TFM and the base is pure rigid.

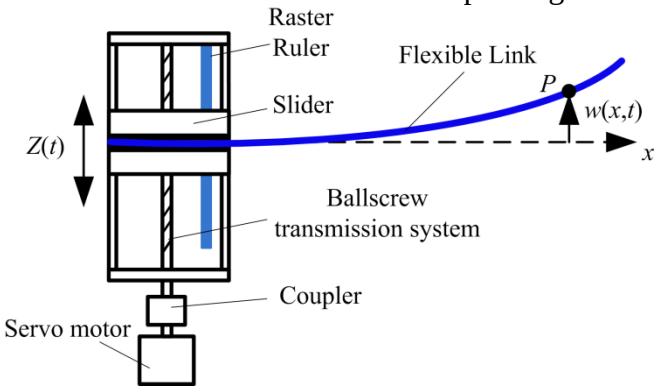

Figure 1: Schematic diagram of the TFM system.

In accordance with the assumed mode methods [13], the axial absolute coordinates of P which is a random point on the TFM can be expressed as:

$$Y(t) = Z(t) + \omega(x,t) = Z(t) + \sum_{i=1}^{i\to\infty} \phi_i(x) q_i(t)\,, \tag{1}$$

where $Z(t)$ is the base displacement, $\omega(x,t)$ denotes the elastic deformation of P, $\phi_i(x)$ is the *ith* modal shape and $q_i(t)$ is the modal coordinates. Owing to the TFM can be considered as a cantilever beam, $\phi_i(x)$ can be further represented as:

$$\phi_i(x) = \sin\beta_i x - \sinh\beta_i x - \frac{\sin\beta_i L_b + \sinh\beta_i L_b}{\cosh\beta_i L_b + \cos\beta_i L_b}(\cos\beta_i x - \cosh\beta_i x), \tag{2}$$

where $\beta_i^4 = \lambda_i^2(\rho A / EI)$, λ_i is the *ith* inherent frequency of the TFM.

Through dynamic analysis of the TFM, the system kinetic energy can be written as:

$$T_e = \frac{1}{2}m_b\dot{Z}^2(t) + \frac{1}{2}\int_0^{L_b}\rho_b A_b\dot{Y}(t)^2 dx, \tag{3}$$

where m_b is mass of the base, ρ_b is density, A_b is the sectional area and L_b is the length of the TFM, respectively.

Potential energy of the system mainly considers the elastic potential energy caused by the elastic deformation of the TFM, and can be expressed as:

$$U_e = \frac{1}{2}\int_0^{L_b} E_b I_b[\frac{\partial^2\omega(x,t)}{\partial x^2}]^2 dx, \tag{4}$$

where E_b and I_b are the elastic modulus and moment of inertia of the TFM, respectively.

The external forces of the TFM primarily include the driving force ($F(t)$) and the friction between the base and the linear guide. So the virtual work of the TFM system is represented by:

$$\sigma W = F(t)\sigma Z(t) - \upsilon_c\dot{Z}(t)\sigma Z(t) - \mu_s\int_0^{L_b}\dot{\omega}(x,t)\sigma\omega(x,t)dx, \tag{5}$$

where υ_c is the friction coefficient between the base and the linear guide and μ_s is the structural damping of the TFM. According to the second Lagrange equation as follows

$$\frac{d}{dt}(\frac{\partial L}{\partial\dot{q}_j}) - \frac{\partial L}{\partial q_j} = Q_j', \tag{6}$$

where Q_j' denotes generalized force which corresponds to generalized coordinates q_j'.

$L = T_e - U$ is Lagrange multiplier and can be expressed as:

$$L = \frac{1}{2}m_b\dot{Z}^2(t) + \frac{1}{2}\int_0^{L_b}\rho_b A_b\dot{Y}(t)^2 dx - \frac{1}{2}\int_0^{L_b} E_b I_b\left[\frac{\partial^2\omega(x,t)}{\partial x^2}\right]^2 dx. \tag{7}$$

With the Lagrange approach and the orthogonality of the modal shape function, the dynamic model of the TFM can be deduced which is showed as:

$$(m_b + \rho_b A_b L_b)\ddot{Z}(t) + \sum_{i=1}^{\infty} m_i\ddot{q}_i(t) = F(t) - v_c\dot{Z}(t), \tag{8}$$

$$m_i\ddot{Z}(t) + \rho_b A_b\ddot{q}_i(t) + \rho_b A_b\lambda_i^2 q_i(t) = 0, \tag{9}$$

where $m_i = \rho_b A_b\int_0^{L_b}\phi_i(x)dx$ is the modal mass.

3. Control Design

The mode numbers have a significant impact on the design of the vibration controller for the TFM. Thus, the selection of the number of modal order has been discussed firstly. The vibration responses of the TFM in our paper with different assumed mode numbers of j are compared in Fig. 2. The results show that when the value of j is greater than 2, the vibration responses rapidly toward stable and the minor change can be neglected. This can be obtained that incorporating the first two modal shapes in the design process of observer and vibration controller is enough and reasonable.

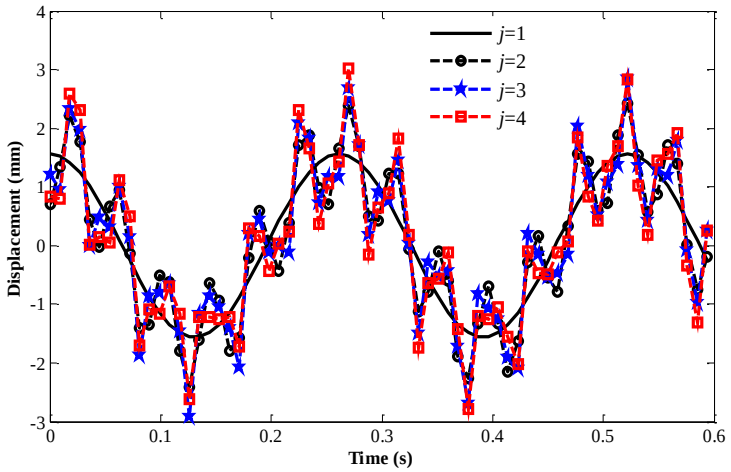

Figure 2: Vibration responses of the TFM with different mode numbers.

Thus, in order to simplify the computation, only the first-two order modes are taken into consideration. Taking the state variables as $\mathbf{x}=[Z \quad q_1 \quad q_2 \quad \dot{Z} \quad \dot{q}_1 \quad \dot{q}_2]^{\mathrm{T}}$, the system dynamic equation can be transformed into the state space equation whose form is

$$\begin{cases} \dot{x} = \mathbf{A}x + \mathbf{B}u \\ y = \mathbf{C}x + \mathbf{D}u \end{cases}, \tag{10}$$

where $\mathbf{A}=\begin{bmatrix} \mathbf{0} & \mathbf{I} \\ \mathbf{M}^{-1}\mathbf{H} & \mathbf{M}^{-1}\mathbf{Q} \end{bmatrix}$, $\mathbf{B}=\begin{bmatrix} \mathbf{0} \\ \mathbf{M}^{-1}\mathbf{\Lambda} \end{bmatrix}$, $\mathbf{C}=\begin{bmatrix} 1 & 0 & \cdots & 0 \\ 0 & 1 & \ddots & \vdots \\ \vdots & \ddots & \ddots & 0 \\ 0 & \cdots & 0 & 1 \end{bmatrix}_{6*6}$, $\mathbf{D}=\begin{bmatrix} 0 \\ \vdots \\ 0 \end{bmatrix}_{6*1}$ and

$$\mathbf{M}=\begin{bmatrix} m_b+\rho_b A_b L_b & m_1 & m_2 \\ m_1 & \rho_b A_b & 0 \\ m_2 & 0 & \rho_b A_b \end{bmatrix},\ \mathbf{H}=\begin{bmatrix} 0 & 0 & 0 \\ 0 & -\rho_b A_b \lambda_1^{\,2} & 0 \\ 0 & 0 & -\rho_b A_b \lambda_2^{\,2} \end{bmatrix},\ \mathbf{\Lambda}=\begin{bmatrix} 1 \\ 0 \\ 0 \end{bmatrix},\ \mathbf{Q}=\begin{bmatrix} -\upsilon_c & 0 & 0 \\ 0 & 0 & 0 \\ 0 & 0 & 0 \end{bmatrix}.$$

Through the analysis of the observability [14], the TFM system is completely observable, which meet the existence conditions of a Luenberger observer. Based on the dynamic model of the TFM in Section 2, the vibration observer is constructed as illustrated in Fig. 3, where $\mathbf{C}_1=[1 \quad 0 \quad 0 \quad 0 \quad 0 \quad 0]$, $\mathbf{C}_2=[0 \quad \phi_1(L_b) \quad \phi_2(L_b) \quad 0 \quad 0 \quad 0]$, $\mathbf{C}_4=[1 \quad \phi_1(L_b) \quad \phi_2(L_b) \quad 0 \quad 0 \quad 0]$ and $\hat{\omega}(L_b,t)$ is denoted as the estimates of $\omega(L_b,t)$.

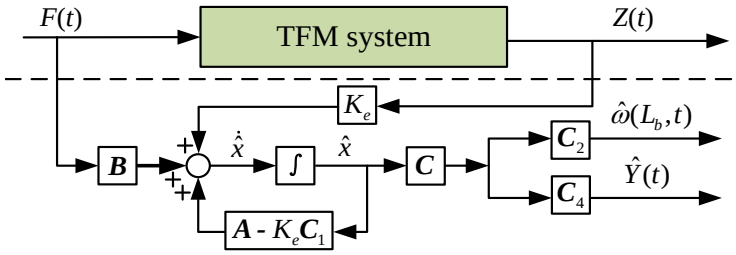

Figure 3: Principle diagram of the vibration observer.

The inputs of the vibration observer are the driving force and the measured displacement of the base. Then, the vibration observer equation can be expressed as:

$$\dot{\hat{x}} = (\mathbf{A}-\mathbf{K}_e\mathbf{C}_1)\hat{x} + K_e Z + \mathbf{B}u, \tag{11}$$

where $\mathbf{K}_e$ is the observer gains matrix. Subtracting Eq. (11) from Eq. (10), the error model of the vibration observer can be obtained as:

$$\dot{\tilde{\mathbf{x}}} = \mathbf{A}\tilde{\mathbf{x}} - \mathbf{K}_e\tilde{Z}, \tag{12}$$

where $\tilde{\Lambda}$ represents the observation error of the corresponding variables.

The design of the observation gains for the vibration observer is based on the thought of no deviation Kalman estimator while keeping the stability of the whole TFM system. The form of $\mathbf{K}_e$ can be written as:

$$\mathbf{K}_e = (\mathbf{R}^{-1}\mathbf{C}_1\mathbf{P})^{\mathrm{T}}, \tag{13}$$

where $\mathbf{R}$ is a positive definite diagonal matrix in Ricatti equation and $\mathbf{P}$ is the positive definite solution of Ricatti equation by defining appropriate $\mathbf{Q}$. The form of Ricatti equation can be shown as:

$$\mathbf{AP} + \mathbf{PA}^{\mathrm{T}} - \mathbf{PC}_1{}^{\mathrm{T}}\mathbf{R}^{-1}\mathbf{C}_1\mathbf{P} + \mathbf{Q} = \mathbf{0}. \tag{14}$$

In order to guarantee the stability of the observer system, the Lyapunov function of the error model is defined as:

$$V = \tilde{\mathbf{x}}^{\mathrm{T}}\mathbf{P}^{-1}\tilde{\mathbf{x}}. \tag{15}$$

Derivation V with respect to time yields:

$$\begin{aligned}
\dot{V} &= \dot{\tilde{\mathbf{x}}}^{\mathrm{T}}\mathbf{P}^{-1}\tilde{\mathbf{x}} + \tilde{\mathbf{x}}^{\mathrm{T}}\mathbf{P}^{-1}\dot{\tilde{\mathbf{x}}} \\
&= [(\mathbf{A} - \mathbf{K}_e\mathbf{C}_1)\tilde{\mathbf{x}}]^{\mathrm{T}}\mathbf{P}^{-1}\tilde{\mathbf{x}} + \tilde{\mathbf{x}}^{\mathrm{T}}\mathbf{P}^{-1}[(\mathbf{A} - \mathbf{K}_e\mathbf{C}_1)\tilde{\mathbf{x}}] \\
&= \tilde{\mathbf{x}}^{\mathrm{T}}\mathbf{A}^{\mathrm{T}}\mathbf{P}^{-1}\tilde{\mathbf{x}} - \tilde{\mathbf{x}}^{\mathrm{T}}\mathbf{C}_1{}^{\mathrm{T}}\mathbf{K}_e{}^{\mathrm{T}}\mathbf{P}^{-1}\tilde{\mathbf{x}} + \tilde{\mathbf{x}}^{\mathrm{T}}\mathbf{P}^{-1}\mathbf{A}\tilde{\mathbf{x}} - \tilde{\mathbf{x}}^{\mathrm{T}}\mathbf{P}^{-1}\mathbf{K}_e\mathbf{C}_1\tilde{\mathbf{x}}. \\
&= \tilde{\mathbf{x}}^{\mathrm{T}}(\mathbf{A}^{\mathrm{T}}\mathbf{P}^{-1} + \mathbf{P}^{-1}\mathbf{A} - \mathbf{C}_1{}^{\mathrm{T}}\mathbf{K}_e{}^{\mathrm{T}}\mathbf{P}^{-1} - \mathbf{P}^{-1}\mathbf{K}_e\mathbf{C}_1)\tilde{\mathbf{x}} \\
&= \tilde{\mathbf{x}}^{\mathrm{T}}\mathbf{P}^{-1}(\mathbf{PA}^{\mathrm{T}} + \mathbf{AP} - \mathbf{PC}_1{}^{\mathrm{T}}\mathbf{K}_e{}^{\mathrm{T}} - \mathbf{K}_e\mathbf{C}_1\mathbf{P})\mathbf{P}^{-1}\tilde{\mathbf{x}}
\end{aligned} \tag{16}$$

Because $\mathbf{Q}$ and $\mathbf{R}$ are symmetric positive definite matrix and $\mathbf{P}$ is positive definite matrix too, $\dot{V}$ is obviously less than zero. Then, the designed vibration observer system is asymptotically stable.

In order to verify the validity of the designed vibration observer, a model of the physical TFM is constructed by ADAMS, which is regarded as a controlled object, and a state-feedback integral controller is designed to suppress the vibrations. The combined-simulation platform of the TFM system is shown in Fig. 4, where $\mathbf{K}_z$ is the feedback gain and K_s is the integral control coefficient.

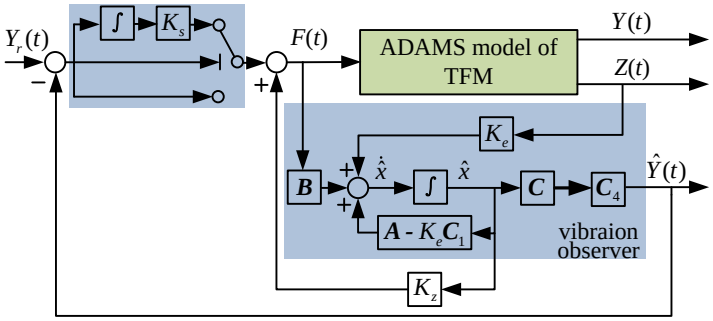

Figure 4: Combined-simulation platform of the TFM system.

If the state feedback controller is used individually, the system static error is inevitable. Then, a judgment link is adopted to make full use of the adjustment ability of the integral controller on the system steady-state error. When the system output is steady, the integral controller is introduced.

The error vector of the TFM system is defined as:

$$\dot{p}(t) = e(t) = Y_r(t) - \hat{Y}(t), \tag{17}$$

where $Y_r(t)$ is the expected displacement for the tip of the TFM.

The state feedback integral control quantity can be represented as:

$$u = \mathbf{K}_z\hat{\mathbf{x}}(t) + K_s\int e(t)dt = \begin{bmatrix}\mathbf{K}_z & K_s\end{bmatrix}\begin{bmatrix}\hat{\mathbf{x}}(t) \\ p(t)\end{bmatrix}. \tag{18}$$

To solving static error, an augmented matrix is introduced and its form is:

$$\begin{cases}\begin{bmatrix}\dot{\hat{\mathbf{x}}}(t) \\ \dot{p}(t)\end{bmatrix} = \begin{bmatrix}\mathbf{A} & 0 \\ -\mathbf{C}_4\mathbf{C} & 0\end{bmatrix}\begin{bmatrix}\hat{\mathbf{x}}(t) \\ p(t)\end{bmatrix} + \begin{bmatrix}\mathbf{B} \\ 0\end{bmatrix}u + \begin{bmatrix}\mathbf{K}_e \\ 0\end{bmatrix}\mathbf{C}_1\hat{\mathbf{x}}(t) + \begin{bmatrix}d(t) \\ Y_r(t)\end{bmatrix} \\ Y(t) = \hat{Y}(t) = \begin{bmatrix}\mathbf{C}_4\mathbf{C} & 0\end{bmatrix}\begin{bmatrix}\hat{\mathbf{x}}(t) \\ p(t)\end{bmatrix}\end{cases}, \tag{19}$$

where $d(t)$ is external distractions. After combining Eq. (18) and Eq. (19), the coalesced result is converted by Laplace transform and can be expressed as:

$$\begin{bmatrix} \dot{\mathbf{x}}(s) \\ \dot{p}(s) \end{bmatrix} = \left(s\mathbf{I} - \begin{bmatrix} \mathbf{A} - \mathbf{K}_e\mathbf{C} + \mathbf{B}\mathbf{K}_z + \mathbf{K}_e\mathbf{C}_1 & \mathbf{B}K_s \\ \mathbf{-C}_4\mathbf{C} & 0 \end{bmatrix} \right)^{-1} \begin{bmatrix} d(s) \\ -Y_r(s) \end{bmatrix}. \tag{20}$$

By the final value theorem, the steady-state value of the system can be calculated as:

$$\lim_{t\to 0} \begin{bmatrix} \mathbf{x}(t) \\ p(t) \end{bmatrix} = \lim_{s\to 0} s\left(s\mathbf{I} - \begin{bmatrix} \mathbf{A} - \mathbf{K}_e\mathbf{C} + \mathbf{B}\mathbf{K}_z + \mathbf{K}_e\mathbf{C}_1 & \mathbf{B}K_s \\ \mathbf{-C}_4\mathbf{C} & 0 \end{bmatrix} \right)^{-1} \begin{bmatrix} d(s)/s \\ -Y_r(s)/s \end{bmatrix} = \begin{bmatrix} \mathbf{A} - \mathbf{K}_e\mathbf{C} + \mathbf{B}\mathbf{K}_z + \mathbf{K}_e\mathbf{C}_1 & \mathbf{B}K_s \\ \mathbf{-C}_4\mathbf{C} & 0 \end{bmatrix}^{-1} \begin{bmatrix} d_0 \\ -Y_{r0} \end{bmatrix} \tag{21}$$

Through analyzing Eq.(21), *p(t)* tends to be constant that means $\dot{p}(t)$ is steady and the final value is zero, so the static error is:

$$\lim_{t\to\infty} \left(Y_r(t) - \hat{Y}(t) \right) = \lim_{t\to\infty} \dot{p}(t) = 0 \cdot \tag{22}$$

As a result of analysis, the specified input of the TFM can be tracked with zero steady-state error based on designing appropriate state feedback integral control law for the augmented matrix.

4. Simulation experiment of the TFM

The material of the TFM is stainless and relevant physical parameters are listed as: L=0.635 m, ρ=7850 kg/m^3, A=28.3e-4 m^2 and E=197 GPa. In order to facilitate the analysis, the ADAMS virtual prototype of the TFM is imported into the MATLAB/Simulink to construct the combined-simulation platform. The outputs of the ADAMS sub-module are the displacement and velocity of the base and the tip of the TFM.

Considering observer response should be faster than the TFM system and the external disturbance, the eigenvalues of observer are generally designed as 2-5 times more than the TFM. Under the consideration of the first-order mode and the first 2-order modes, the observer gains are set as [48.00 –43.27 556.8 –832.28] and [30.44 –51.63 5.25 –5.76 127.42 347.63]. The total simulation time is 3 s and the simulation step is 0.001 s. The motion of the base is defined as constant acceleration when t=0~0.8 s, constant speed when t=0.8~1.6 s and constant deceleration when 1.6s~2.4s.

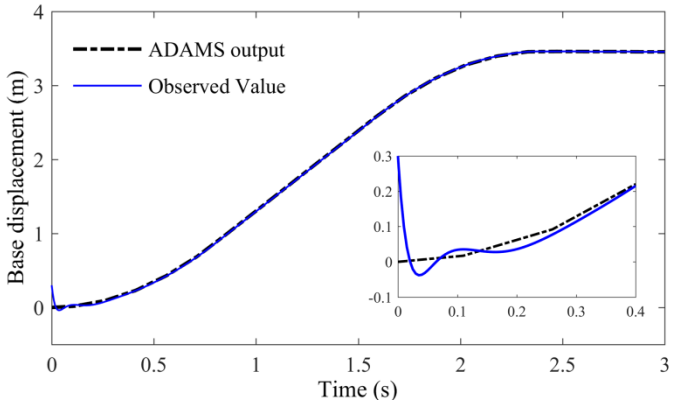

Figure 5: Tracking effect of base displacement.

Figures 5-6 show the tracking effect of the base displacement and velocity by the designed vibration observer. It can be seen that the vibration observer can accurately track the base displacement and velocity under the movement of constant acceleration and constant speed. The tracking speed of the base displacement is high and the initial disturbances can be quickly eliminated.

Figure 7 shows the tracking effect for the tip vibrations of the TFM. The tracking trend of the tip vibrations, which is very significant to control, is consistent with the output of ADAMS in a very short period of time whether considering the first-order mode or the first 2-order modes. Also there is a certain deviation on the amplitude. The fact that the amplitude error of the observation results

decreased with the increase of the mode order numbers demonstrates that the observation error is caused by the mode truncation, which is consistent with the theoretic analysis. The only difference between the first-order mode and the first 2-order modes is slight amplitude deviation, which further proves the effectiveness of the proposed observer.

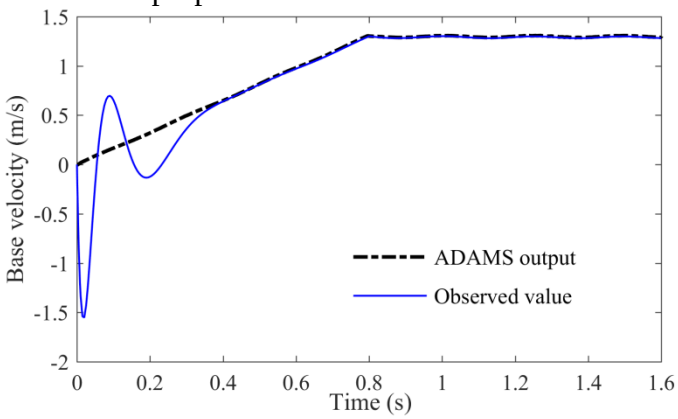

Figure 6: Tracking effect of base velocity.

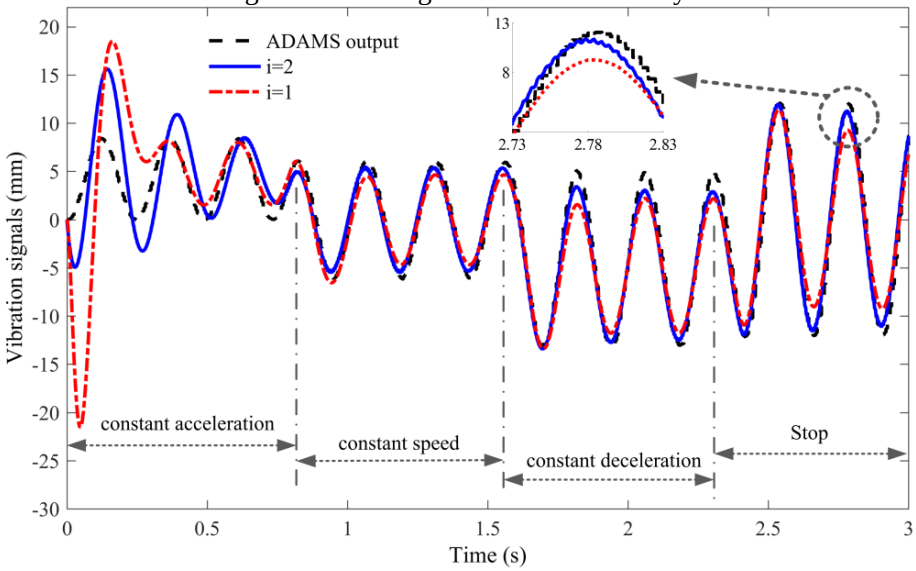

Figure 7: Tracking effect of tip vibrations of the TFM.

By setting the desired output as $Y_r = 0.1$ m which means that when the base moves to 0.1 m, the vibrations of tip rapidly decay to 0, the control results are shown in Fig. 8. Where SFIC indicates the state feedback integral controller and FAT means the free attenuation of the tip vibrations for only positioning the base to the desired point.

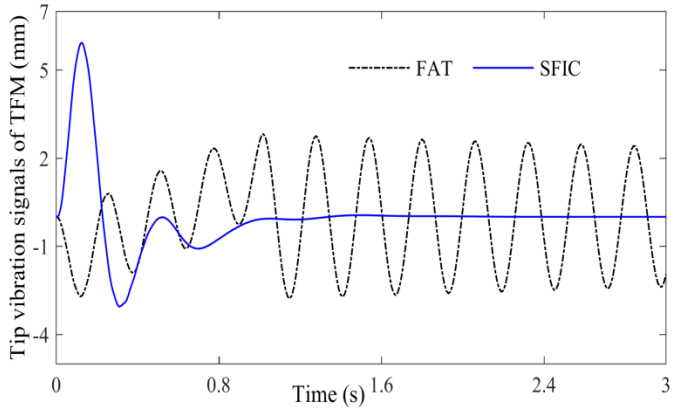

Figure 8: Control effect of tip vibrations of the TFM.

The results shown in Fig. 8 indicate that the SFIC is effective. The tip vibration signals of the TFM attenuate to 0 since 1.4s. Because the control force is based on the observed values, the validity of the designed vibration observer can be further proved.

5. Conclusions

This paper investigates sensor-less measurement of the vibration signals for a TFM system. The vibration observer is constructed by the Lumped parameter dynamic models of the TFM. Then a physical model of the TFM is established by ADAMS software to verify the effectiveness of the designed methods. Results show that the designed vibration observer has a noticeable effect of vibration observation during the constant acceleration, constant speed and constant deceleration motion of the base. Additionally, the vibration observer can also effectively estimate the residual vibration for the tip of the TFM after the base movement stops. Moreover, the state feedback integral controller can effectively restrain the residual vibration of the TFM and improve the position precision of the whole system. By replacing the sensors to observers, the sensors' disadvantages of inconvenience of installation and the influence on the system dynamic characteristics can be avoided. Meanwhile, it has positive significance for the structural optimization and cost reduction. Thus, in industrial control, aerospace and other fields, the application of observers will be more extensive in future.

Acknowledgements

This work was partially supported by the National Natural Science Foundation of China (No. 51305444), the Postgraduate Cultivation and Innovation Project of Jiangsu Province (KYZZ16-0213), and the Project Funded by the Priority Academic Program Development of Jiangsu Higher Education Institutions (PAPD).

REFERENCES

1 Brogårdh, T. Present and future robot control development—An industrial perspective, *Annual Reviews in Control*, **31**(1):69-79, (2007).

2 Li, Z. and Du, R.X. Design and Analysis of a Bio-Inspired Wire-Driven Multi-Section Flexible Robot Regular Paper, *International Journal of Advanced Robotic Systems*, **10**(10), 209-220, (2013).

3 Katsura, S. and Ohnishi, K. Force Servoing by Flexible Manipulator Based on Resonance Ratio Control, *IEEE Transactions on Industrial Electronics*, **54**(1), 539-547, (2007).

4 Kiang, C.T., Spowage A. and Yoong C.K. Review of Control and Sensor System of Flexible Manipulator, *Journal of Intelligent & Robotic Systems*, **77**(1), 187-213, (2015).

5 Qiu, Z.C. Adaptive nonlinear vibration control of a Cartesian flexible manipulator driven by a ball screw mechanism, *Journal of Mechanical Systems*, **30**(7), 248-266, (2012).

6 Malki, H.A. and Misir, D. Fuzzy PID control of a flexible-joint robot arm with uncertainties from time-varying loads, *IEEE Transactions on Control Systems Technology*, **5**(3), 371-378, (1997).

7 João C.P.R. and José S.D.C. Motion planning and actuator specialization in the control of active-flexible link robots, *Journal of Sound and Vibration*, **331**(14), 3255-3270, (2012).

8 Yoo, S.J., Park, J.B. and Choi, Y.H. Adaptive output feedback control of flexible-joint robots using neural networks: dynamic surface design approach, *IEEE Transactions on Neural Networks*, **19**(10), 1712-1726, (2008).

9 Gudiño-Lau, J., Arteaga, M.A., Munoz, L.A. and Parra-Vega, V. On the control of cooperative robots without velocity measurements, *IEEE Transactions on Control Systems Technology*, **12**(4), 600-608, (2004).

10 Tavasoli, A., Eghtesad, M. and Jafarian, H. Two-time scale control and observer design for trajectory tracking of two cooperating robot manipulators moving a flexible beam, *Robotics and Autonomous Systems*, **57**(2), 212-221, (2009).

11 Mosayebi, M., Ghayour, M. and Sadigh, M.J. A nonlinear high gain observer based input–output control of flexible link manipulator, *Mechanics Research Communications*, **45**, 34-41, (2012).

12 Davide, S. and Daniel, J. Distributed Full-State Observers With Limited Communication and Application to Cooperative Target Localization, *Journal of Dynamic Systems, Measurement, and Control*, **136**(3), 031022, (2014).

13 Mirzaee, E., Eghtesad, M. and Fazelzadeh, S.A. Maneuver control and active vibration suppression of a two-link flexible arm using a hybrid variable structure/Lyapunov control design, *Acta Astronautica*, **67**(67), 1218-1232, (2010).

14 Morales, R., Feliu, V. and Jaramillo, V. Position control of very lightweight single-link flexible arms with large payload variations by using disturbance observers, *Robotics and Autonomous Systems*, **60**(4), 532-547, (2012).